Supporting information for

A prototype of high-performance two-electron non-aqueous organic redox flow battery operated at -40 °c

Zhiming Liang[a,c]*, Rahul kant Jha[a,b], Thilini Malsha Suduwella[a,b], N. Harsha Attanayake[a,b], Yangyang Wang[c], Wei Zhang[c], Chuntian Cao[d], Aman Preet Kaur[a,b], James Landon[e,f], and Susan A. Odom[a,b]

[a] Department of Chemistry, University of Kentucky, Lexington, KY 40506, USA
[b] Joint Center for Energy Storage Research, Lexington, KY 40506, USA
[c] Department of mechanical Engineering, University of Colorado, Boulder, CO 80309, USA
[d] Computational Science Initiative, Brookhaven National Laboratory, Upton, NY 11973, USA
[e] Center for Applied Energy Research, University of Kentucky, Lexington, KY 40511, USA
[f] Department of Chemical and Materials Engineering, University of Kentucky, Lexington, KY 40506, USA

* Corresponding author information
leungchiminh@gmail.com

Figures and Tables

Table S1. Progress of aqueous and non-aqueous redox flow batteries at low temperature.

Aqueous inorganic RFBs							
catholyte	anolyte	cycled temperature	active materials concentration	cell voltage	cycled current (mA cm^{-2})	accessed capacity	Refs.
Zn/Zn^{2+}	I_3/I^-	-20 °C	3.5 M	~ 1.3 V	10 (40 cycles)	~ 130 Ah L^{-1}	[1]
$FeCl_2$	MeTsPc	-30 °C	0.05 M	~ 1.3 V	3 (50 cycles)	~ 1.5 Ah L^{-1}	[2]
VO^{2+}/VO_2^+	$H_6P_2W_{18}O_{62}$	-20 °C	0.5 M	~ 1.1 V	160 (800 cycles)	~ 80 Ah L^{-1}	[3]

Non-aqueous organic RFBs							
catholyte	anolyte	cycled temperature	active materials concentration	cell voltage	current	accessed capacity	Refs.
$H_2TPP/[H_2TPP]^{2+}$	$[H_2TPP]^{2-}/H_2TPP$	-40 °C	0.3M	symmetric cell	1 (~ 200 cycles)	~ 1.8 Ah L^{-1}	[4]
BMEEOEPT	MEEV-$TFSI_2$	-40 °C	0.1M, 0.25M	~ 1.9 V	15 (>100 cycles)	~ 3.2 Ah L^{-1} (0.1M); ~ 8.5 Ah L^{-1} (0.25M)	This work

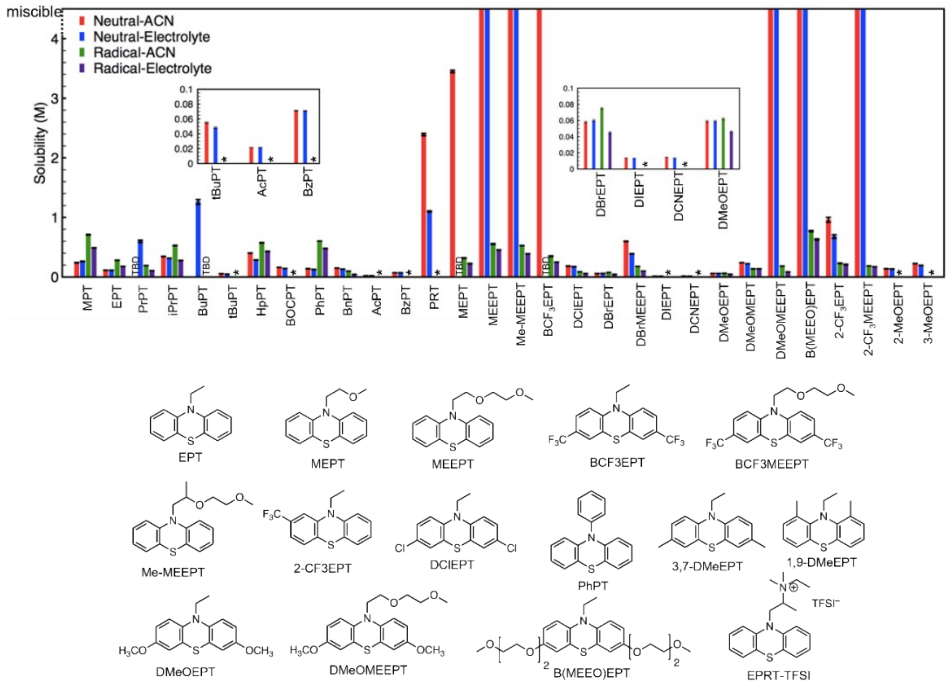

Figure S1. Measured solubility of Phenothiazine derivatives (neutral and radicals) in solvent (ACN) and electrolyte (0.5M $TEABF_4$/ACN). This figure was modified based on our previous research.[5] Reprinted with permission. Copyright The Royal Society of Chemistry.

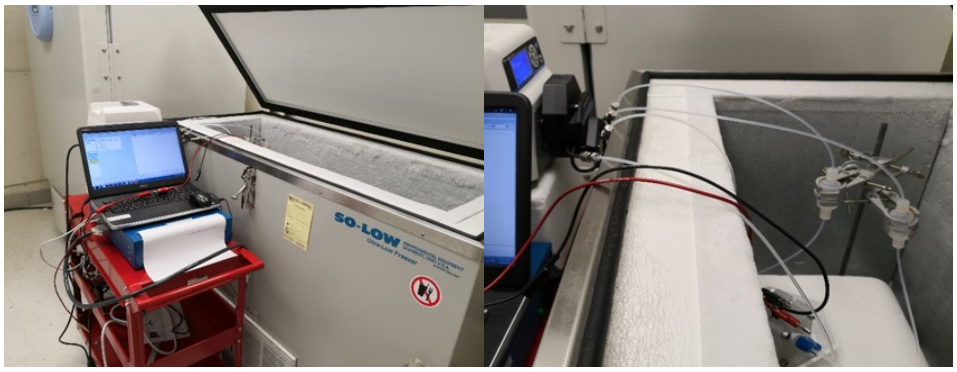

Figure S2. Photographs of the - 40 °C non-aqueous redox flow cell setup.

Table S2. Chemical and electrochemical properties of the commonly used solvents for non-aqueous redox flow battery.[6, 7]

	Melting point (°C)	Boiling point (°C)	Viscosity (mPa s^{-1})*	Electrochemical window (V)
Acetonitrile	-46	81.6	0.34	6.1
Dichloromethane	-96.7	39.6	0.44	N/A
tetrahydrofuran	-108.4	66	0.46	N/A
Propylene carbonate	-48.8	242	0.41	6.6
Dimethoxyethane	-58	85	1.1	N/A
Toluene	-95	111	0.55	N/A
Dimethylformamide	-60	153	0.92	N/A

** Viscosity was measured at 25 °C.*

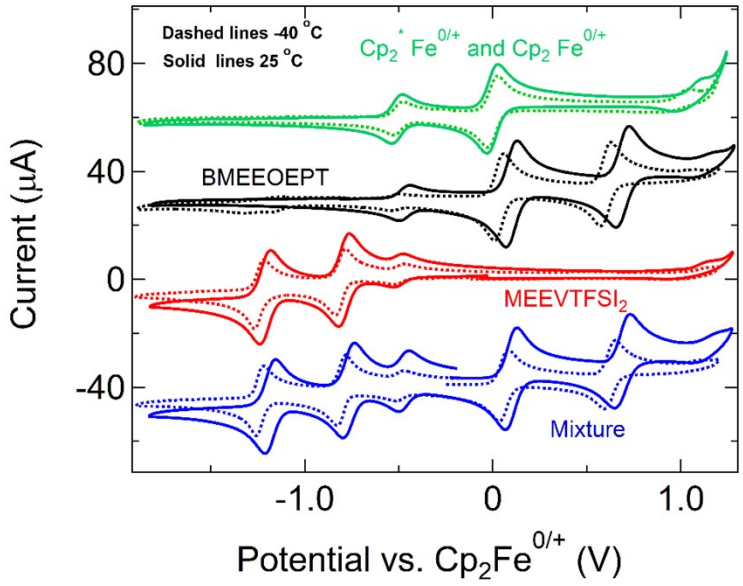

Figure S3. The calibration of the redox potentials using decamethylferrocene and ferrocene (green). In subsequent scans, decamethylferrocene (Cp_2*Fe) was used as an internal reference. Cyclic voltammograms full redox potentials at 25 °C (solid line) and -40 °C (dashed line) of 1 mM BMEEOEPT (black), MEEV-$TFSI_2$ (red), and the combination of BMEEOEPT and MEEV-$TFSI_2$ (blue) in 0.5 M TEATFSI/ACN, all containing decamethylferrocene as an internal reference. The potential of Cp_2*$Fe^{0/+}$ vs. $Cp_2Fe^{0/+}$ is -0.509 V (25 °C) and -0.515 V (-40 °C). All scans are calibrated to ferrocene/ferrocenium ($Cp_2Fe^{0/+}$) at 0 V. The scan rate was 100 mV s^{-1}.

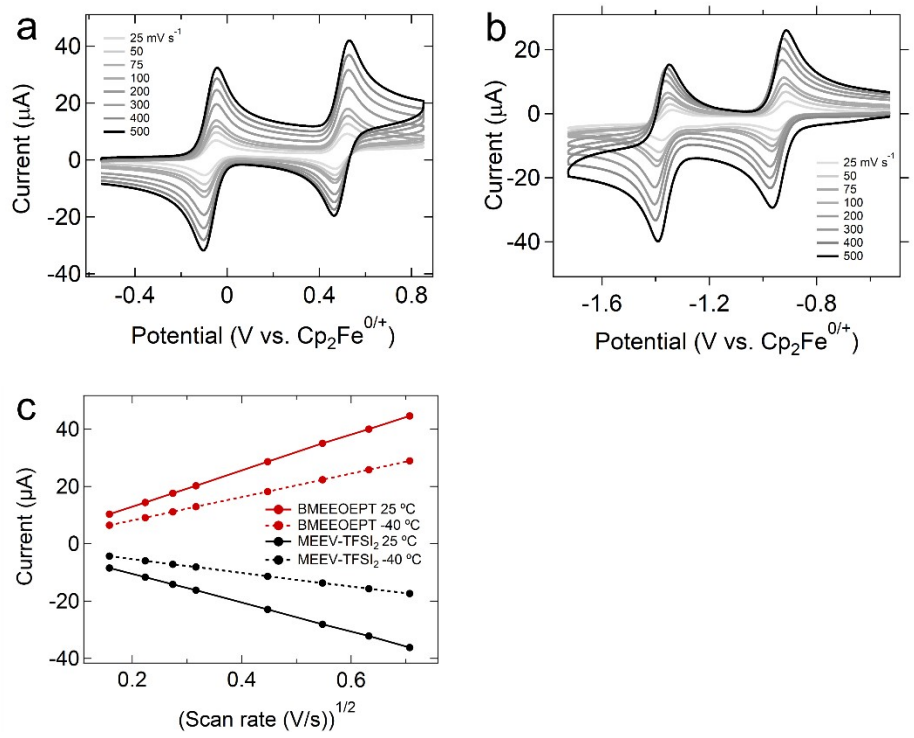

Figure S4. CV of 1 mM BMEEOEPT (a) and MEEV-$TFSI_2$ (b) in 0.5 M TEATFSI/ACN at -40 °C; c) The corresponding Randles-Sevcik plot of 1 mM BMEEOEPT and MEEV-$TFSI_2$. The Scan rates are 25, 50, 75, 100, 200, 300, 400, and 500 mV s^{-1}.

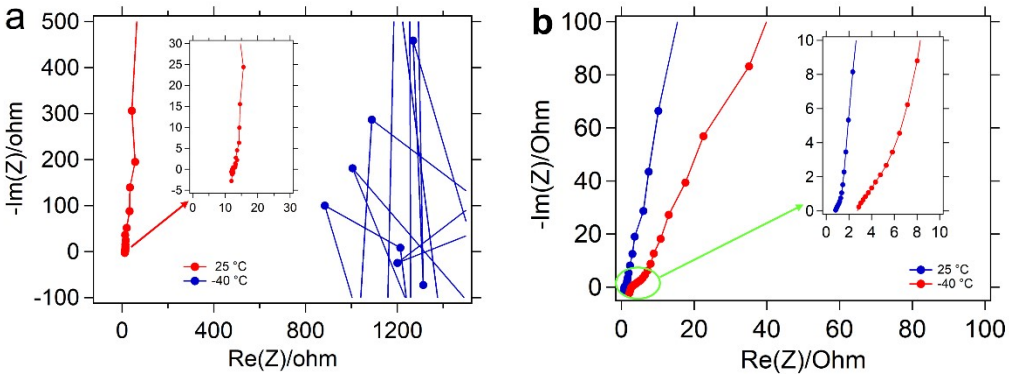

Figure S5. Nyquist plots of 2X FAPQ 375 PP (a) and Daramic 175 separator in 0.5M TEATFSI/ACN at 25 and -40 °C. The area of tested membrane or separator is 2.55 cm^2. EIS was conducted with circulating electrolytes with an amplitude of 10 mV in a frequency range of 100 kHz to 1Hz (5 steps per decade).

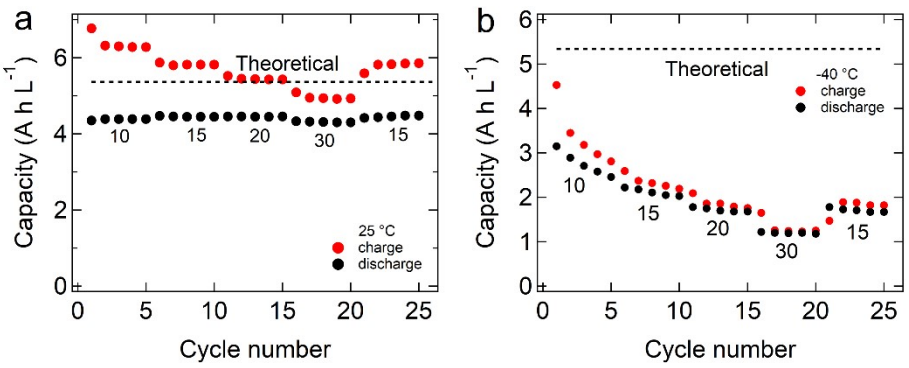

Figure S6. Rate study of the 0.1M premixed cells cycled at 25 (a) and -40 °C (b) with current density of 10, 15, 20, 30, and 15 mA cm^{-2}. The theoretical capacity is 5.36 A h L^{-1}.

Table S3. Electrochemical data of the 0.1M premixed cells cycled at 25 and -40 °C with current density 10, 15, 20, 30, and 15 mA cm^{-2}. Data was calculated by the average of 2^{nd}, 3^{rd}, and 4^{th} cycle at each current density.

Temperature (°C)	current density (mA cm^{-2})	charge capacity (A h L^{-1})	discharge capacity (A h L^{-1})	CE (%)	EE (%)	VE (%)
-40	10	3.2	2.73	85.3	67.2	78.8
	15	2.32	2.11	91.1	65.1	71.5
	20	1.84	1.71	93.1	59.1	63.5
	30	1.24	1.2	96.3	51.8	53.8
	15	1.86	1.7	91.5	64.5	70.5
25	10	6.3	4.39	69.6	58.3	83.8
	15	5.81	4.45	76.7	62.9	82
	20	5.44	4.45	81.9	64.9	79.2
	30	4.94	4.31	87.4	63.6	72.8
	15	5.83	4.46	76.4	62.9	82.3

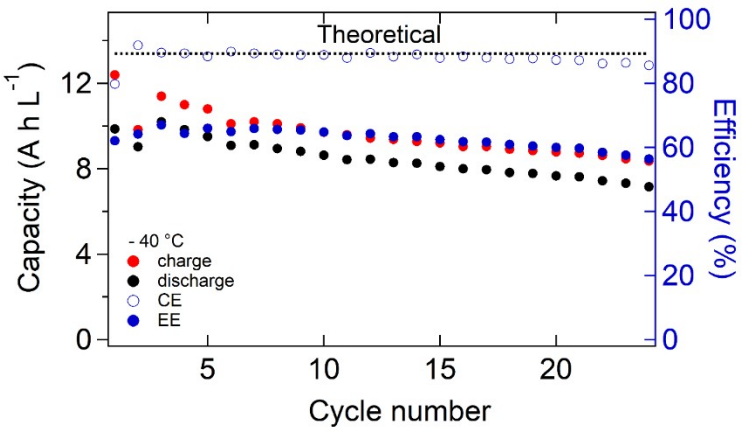

Figure S7. -40°C 0.25 M premixed BMEEOEPT and MEEV-$TFSI_2$ cell with Daramic 175 separator. The current rate is 15 mA cm^{-2}. The theoretical capacity is 13.4 A h L^{-1}.

Table S4. Fitting EIS data for the 25 and -40 °C cells. R_1 stands for ohmic resistance. R_2 stands for charge transfer resistance.

	before cycling 25 °C	after 100 cycles 25 °C	before cycling - 40 °C	after 100 cycles - 40 °C	move to 25 °C
R_1 (Ω)	0.872	0.889	2.11	2.792	1.626
R_2 (Ω)	2.736	0.136	6.467	0.9616	0.247

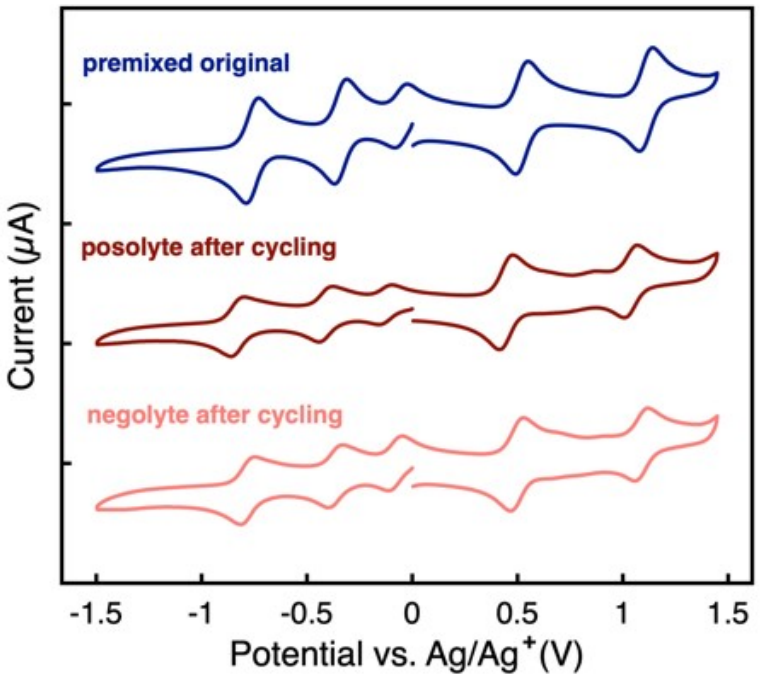

Figure S8. CV of 0.1M premixed -40 °C cell before and after cycling vs Ag/Ag^{+}. Decamethylferrocene was used as the internal reference. The scan rate is 100 mV s^{-1}.

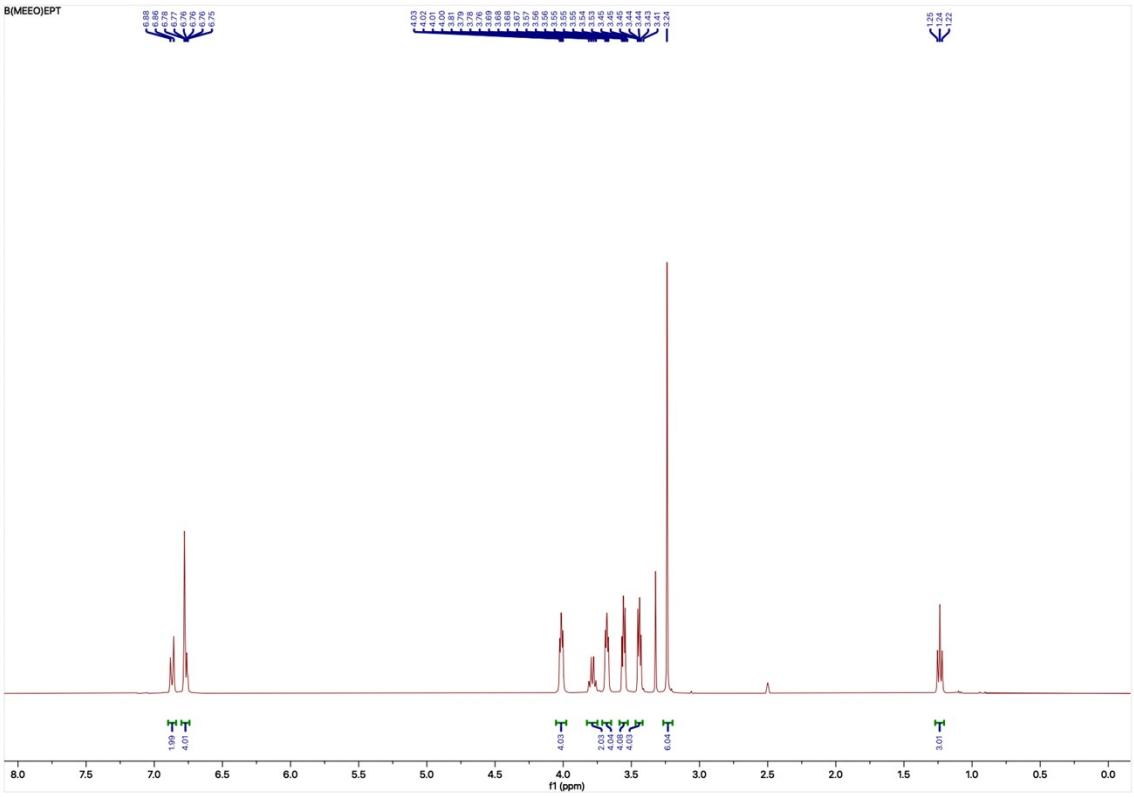

Figure S9. Pristine N-ethyl-3,7-bis(2-(2-methoxyethoxy)ethoxy)phenothiazine (BMEEOEPT). ^{1}H NMR (DMSO-d6, 400 MHz, ppm) δ 6.88 (d, J = 9.7 Hz, 2H), 6.79 – 6.75 (m, 4H), 4.04 – 3.98 (m, 4H), 3.79 (q, J = 6.9 Hz, 2H), 3.71 – 3.65 (m, 4H), 3.58 – 3.52 (m, 4H), 3.47 – 3.42 (m, 4H), 3.24 (s, 6H), 1.24 (t, J = 6.8 Hz, 3H).[8]

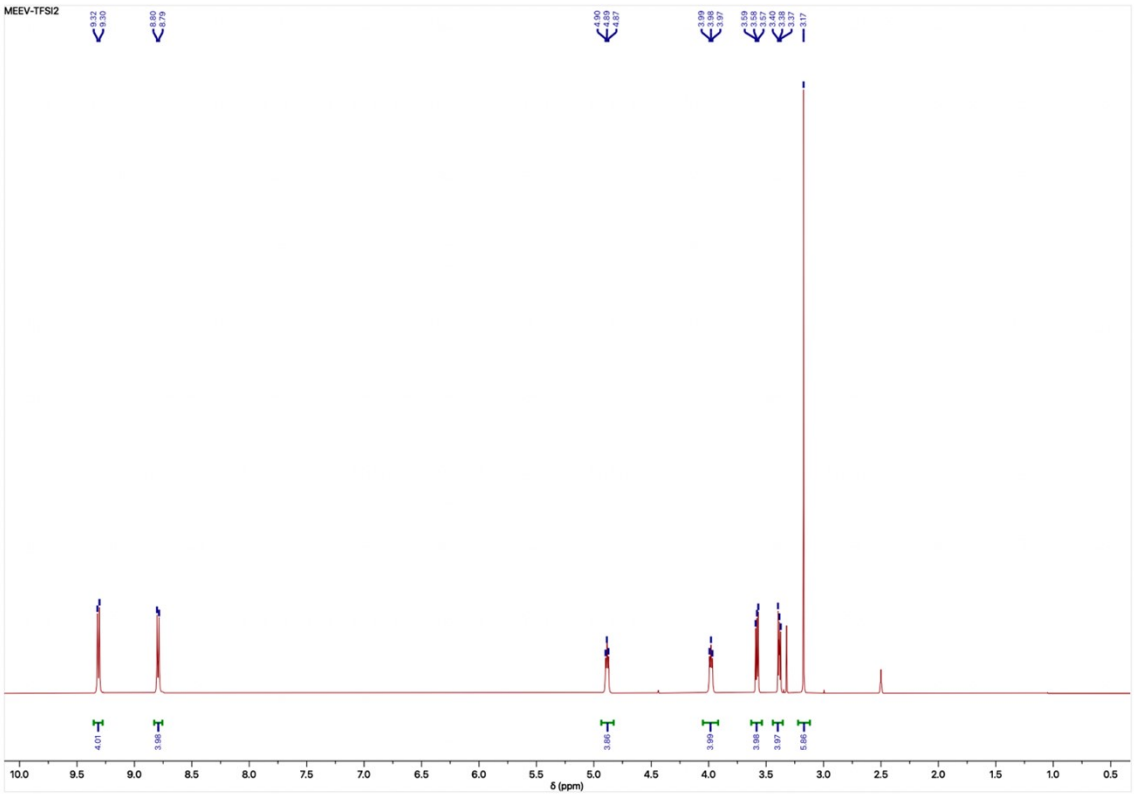

Figure S10. Pristine Bis((2-(2-methoxyethoxy)ethyl))viologen bis(trifluoromethanesulfonyl)imide (MEEV-$(TFSI)_2$). ^{1}H NMR (DMSO-d_6, 400 MHz, ppm) δ 9.3 (d, J = 6.6 Hz, 4H), 8.78 (d, J = 6.6 Hz, 4H), 4.88 (t, J= 5.0 Hz, 4H), 4.00 (t, J = 5Hz, 4H), 3.57 (t, J = 4.4 Hz, 4H), 3.38 (t, J = 4.4 Hz, 4H), 3.17 (s, 6H).[9]

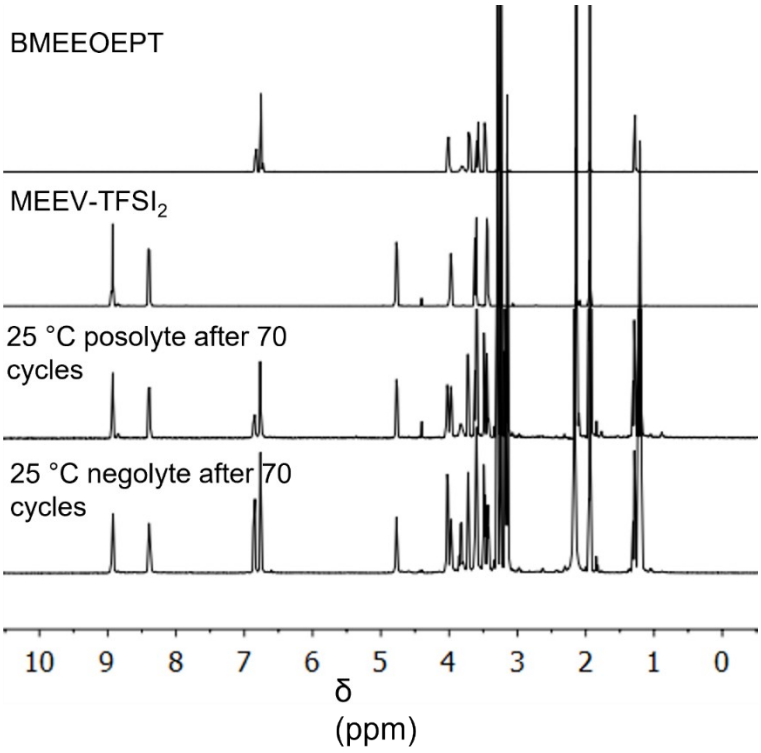

Figure S11. ^{1}H NMR spectra of 0.5 M BMEEOEPT and MEEV-$TFSI_2$ separated cell assembled with 2x FAPQ 375 PP membrane before and after 70 cycles (CD_3CN, 400 MHz) at 25 °C.

References

1. B. Li, Z. Nie, M. Vijayakumar, G. Li, J. Liu, V. Sprenkle and W. Wang, *Nat. Commun.*, 2015, **6**, 1-8.
2. Z. Huang, P. Zhang, X. Gao, D. Henkensmeier, S. Passerini and R. Chen, *ACS Appl. Energy Mater.*, 2019, **2**, 3773-3779.
3. F. Ai, Z. Wang, N.-C. Lai, Q. Zou, Z. Liang and Y.-C. Lu, *Nat. Energy*, 2022, **7**, 417-426.
4. T. Ma, Z. Pan, L. Miao, C. Chen, M. Han, Z. Shang and J. Chen, *Angew. Chem. Int. Ed.*, 2018, **57**, 3158-3162.
5. A. S. Perera, T. M. Suduwella, N. H. Attanayake, R. K. Jha, W. L. Eubanks, I. A. Shkrob, C. Risko, A. P. Kaur and S. A. Odom, *Mater. Adv.*, 2022, DOI: 10.1039/D2MA00598K.
6. K. Gong, Q. Fang, S. Gu, S. F. Y. Li and Y. Yan, *Energy Environ. Sci.*, 2015, **8**, 3515-3530.
7. J. Barthel, R. Neueder and H. Roch, *J. Chem. Eng. Data*, 2000, **45**, 1007-1011.
8. N. H. Attanayake, J. A. Kowalski, K. V. Greco, M. D. Casselman, J. D. Milshtein, S. J. Chapman, S. R. Parkin, F. R. Brushett and S. A. Odom, *Chem. Mater.*, 2019, **31**, 4353-4363.
9. N. H. Attanayake, Z. Liang, Y. Wang, A. P. Kaur, S. R. Parkin, J. K. Mobley, R. H. Ewoldt, J. Landon and S. A. Odom, *Mater. Adv.*, 2021, **2**, 1390-1401.